IEEE Region 10 Conference on Computer and Communication Systems, September 1990, Hong Kong

Fingerprint Image Processing Using Neural Network

Ming-Tak LEUNG
Space, Telecommunication &
Radioscience Laboratory
Stanford Unviersity
Stanford, California, U.S.A.

W. E. ENGELER and P. FRANK
Electronic System Laboratory
General Electric, CRD
Schenectady, New York, U.S.A.

Abstract:

A system for minutiae extraction in fingerprint images using back-propagation networks and Gabor filters is described. Fingerprint images are first convolved with complex Gabor filters and the resulting phase and magnitude signals are passed to networks to identify minutia regions. Promising results are obtained with good detection ratio and low false alarm rate. The importance of having good representations of image data to neural networks is illustrated through variations in performances of different trained networks. The usefulness of Gabor filters in textural image processing and neural networks in image feature extraction are demonstrated.

1. Introduction

In the electrical engineering community there has been a continuing interest in adaptive networks since the early 1960's. [1] The relation of these networks to biological neuron structures, which can also adapt through learning, was understood at that time. The ability of the networks to adapt or be trained beyond a single layer was limited by the adaptive algorithms of that time. In recent years, there has been reviewed interest in this field. This is due to the advances made in the training of multi-layer networks. [2]

Artificial neural networks have found application in a wide range of areas from playing backgammon [3], detecting explosive [4], applications in separating sonar signals [5], reading English text [6], to high energy physics applications [7].

The usefulness of this network architecture in the real work of biology is apparent, as human system can still out-performed any supercomputer in the world when applied to problems such as feature extraction and pattern recognition. In fact, the neural network architecture is most useful when applied to those areas which are easy for humans but difficult for computers. In the paper, the problem of fingerprint minutiae extraction using Gabor filters and back-propagation networks is investigated.

An important issue in applying neural networks to image recognition or processing problems is the representation of image data as input to the network. This is the most computationally intensive portion of the process and therefore for practical system, some form of data reduction must be performed. We prefer to call this the representation layer of the network.

The paper is organized into 6 sections. This introduction serves as the first section. Section 2 will discuss the motivation and configuration of the processing system while Section 3 will discuss the Gabor transform and representation issues. Section 4 describes in more detail the filtering and training procedures involved and the difficulties encountered. Results are given and discussed in Section 5 and the report will end with a brief conclusion section.

2. Processing System

Fingerprints have long been used in the identification of individuals because of the well-known fact that each person has a unique fingerprint. Classification is usually performed by noting the positions of certain features in fingerprint. One of these, known as minutiae, are places where the fingerprint ridges end or are bifurcated. Fig. 1 is a portion of a fingerprint containing a minutiae. In this case, it is in the center of the figure and is a ridge ending of a vertical ridge. Existence, position and orientation of the minutiae are the parameters to be extracted.

The required information, clearly, is contained in the phase changes of the ridges across the print. The representation layer should be some form of frequency transform and have the ability to provide localized information. Gabor filters are chosen to form this representation layer and these filters will be described more fully in the next section. The particular choice of using Gabor filters to perform the representational task is partially inspired by neurophysiological measurements of the two-dimensional anisotropic receptive field profiles describing single neurons in mammalian visual cortex. These field profiles can be captured by the family of Gabor filters using suitable parameters.

An important point to note here is that just like other layers in a neural network, the representation layer may be considered as a remapping and filtering of the preprocessed data. In this case, we may view the filters as networks with pre-specified weights as they perform the same inner product summations as trained back-propagation networks do.

The block diagram of the minutiae extraction system is given in Fig 2. The grey-scale fingerprint picture is first passed through a rank of Gabor filters. Each filter corresponds to a specific orientation of the minutiae to be extracted. Outputs from the filters are then subsampled and passed to a 3-layered back-propagation network with the final output identifying whether minutiae are present or not.

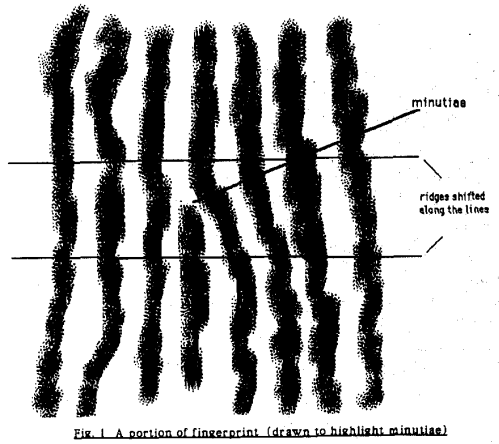

Fig. 1 A portion of fingerprint (drawn to highlight minutiae)

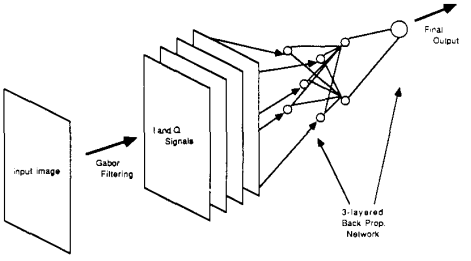

Fig. 2 Block diagram of the minutiae extraction system

3. Gabor Filters Representation Layer

The general functional form of the 2-D Gabor filter family is specified in Eq. 1,2,3 and 4, where h(x,y) is the spatial impulse response and H(u,v) is the 2-D Fourier transform of h(x,y):

$$h(x;y) = g(x',y') \exp(2\pi j F x') \quad (1)$$

$$\text{where} \quad (x',y') = (x\cos\phi + y\sin\phi, -x\sin\phi + y\cos\phi) \quad (2)$$

$$g(x,y) = ab \exp(-a^2x^2 - b^2y^2) \quad (3)$$

$$\text{and} \quad H(u,v) = \pi \exp\{-\pi^2[(u'-F)^2/a^2 + v^2/b^2]\} \quad (4)$$

The filter h(x,y) is characterized by the parameters F, ø, a and b where F and ø correspond to the center frequency and orientation of the filter, while a and b are the scaling parameters. An important property of 2-D Gabor filters is that they achieve the theoretical lower bound of the joint uncertainty in the two conjoint spatial, (x,y), and frequency, (u,v), domains. [8] Defining uncertainty Δ(.) to be the normalized second moments about the principal axes, it can be shown that:

$$\Delta(x)\,\Delta(y)\,\Delta(u)\,\Delta(v) \geq 1/16\pi^2 \quad (5)$$

with the lower bound of Eq. 5 being achieved by the family of Gabor filters. In other words, Gabor filters can have very narrow passbands with optimal spatial locatization.

Interesting results are obtained using Gabor filters for texture segmentation [9][11]. Assuming regions of an image with similar texture, t(x,y), be described as containing only a narrow range of frequencies concentrated at a spatial frequency (F,ø):

$$t(x,y) = 2[c(x,y)\cos(2\pi Fx') + s(x,y)\sin(2\pi Fx')] \quad (6)$$
$$= 2\,e(x,y)\cos[2\pi Fx' + p(x,y)]$$

where (x',y') be defined as in Equ. 2 and e, p are slowly varying amplitude and phase terms.
The convolving of t(x,y) with the Gabor filter h(x,y) will give $k(x,y) = k_I(x,y) + jk_Q(x,y)$ where

$$k_I(x,y) = \quad (7)$$
$$[g(x',y')*c(x,y)]\cos(2\pi Fx') + [g(x',y')*s(x,y)]\sin(2\pi Fx')$$
$$\& \quad k_I(x,y) = \quad (8)$$
$$[g(x',y')*c(x,y)]\sin(2\pi Fx') - [g(x',y')*s(x,y)]\cos(2\pi Fx')$$

From Equ 7 and 8, a slightly modified version of e and p can be obtained by taking magnitude and the phase of the I and Q signals after demodulating them back to baseband with an $\exp(-j2\pi Fx')$ signal.

A major aspect of the system is its input dimension. Suppose we are looking at a window of 32x32 pixels. If we just pass all the pixels into the network, the input vector dimension will be about 1000. It is virtually impossible to train the network as it will involved too much computation. As we have already discussed, some type of reduced representation of the original data is necessary to limit the dimension of the network. The reduced representation must preserve the identifying characteristics of the features to be extracted.

Suppose we have a Gabor filter tuned to ridges running in the vertical direction as in Fig. 1. All portions of that figure will match closely to the Gabor filter mentioned, except the area around the minutiae. So, a dark dot in the center of a bright surround in magnitude of the filtered output is a signature of the minutiae. Consider next the phase of the spatial wave going across the figure, the phase of the waves above and below the minutiae area are different. Ridges are shifted spatially due to the introduction of an additional ridge. This phase shift is therefore also a signature of the minutia. The minutia location should therefore also be characterized by regions where there are significant phase changes.

Referring back to Eq. 7 & 8, the characteristics of minutiae are preserved in the baseband phase and magnitude of the Gabor transform of the fingerprint image. As phase and magnitude signal are more slowly-varying than the original image, subsampling of the filtered image is now possible. This reduces the input vector dimension to the neural network and makes the computation and training of networks feasible.

4. Image Filtering and Network Training

Gabor Filtering

A typical grey-scale image of a fingerprint is shown in Fig. 3 with squares highlight minutiae in the vertical direction. [11] According to Eq. 1, 2 and 3, there are four parameters of the Gabor filter that must be adjusted to tune the filter to fingerprint images. The parameters are the pitch central frequency, F, the orientation, ø, and the scaling parameters, a and b. These determine the spatial extent of the filter and in turn, its spatial bandwidth. Parameters were chosen to maintain a passband wide enough to accommodate pitch frequency variations for different fingerprint images.

It was decided to use filters at six different orientations spaced at a 30 degree interval to identify and classify minutiae into six different orientations. The six filters have responses that sum up to give a uniform total response in all orientations. Minutiae with any orientation would then have an equal chance of being detected by one or an adjacent pair of filters. The spatial impulse response of the Gabor filter pair (real and imaginary) with ø = 0 is given Fig. 4. The window size chosen was 16 x 16, which is a few times the wavelength of fingerprint ridges.

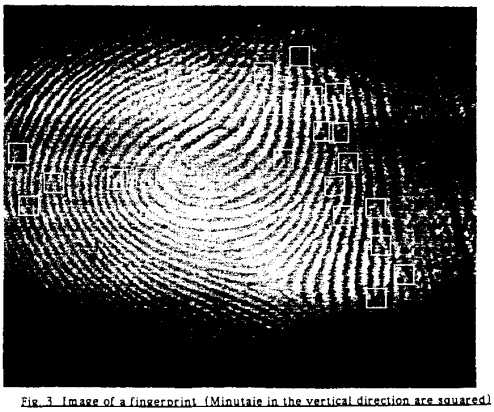

Fig. 3 Image of a fingerprint (Minutaie in the vertical direction are squared)

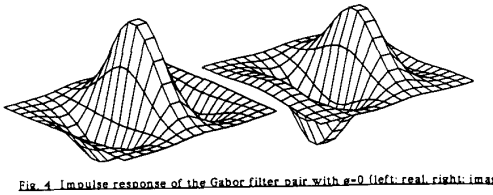

Fig. 4 Impulse response of the Gabor filter pair with ø=0 (left: real, right: imag.)

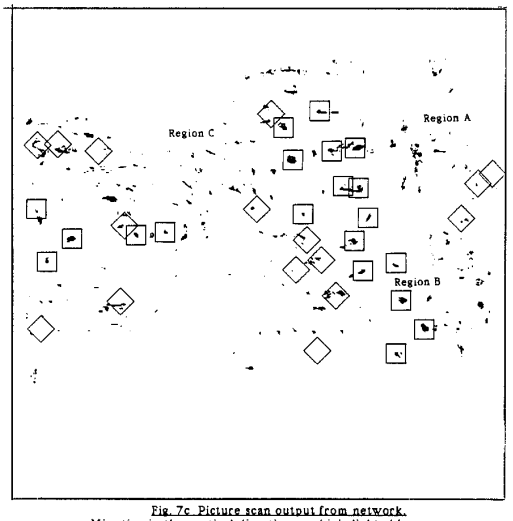

Fig. 7c Picture scan output from network.
Minutiae in the vertical direction are high-lighted by squares.
Minutiae in the two adjacent directions are high-lighted by diamonds.

Fig. 8a Magnitude of filtered output with scaling

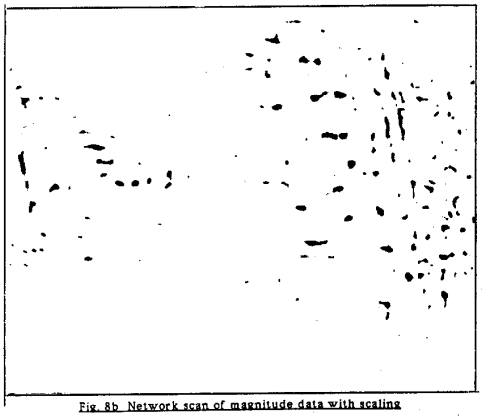

Fig. 8b Network scan of magnitude data with scaling

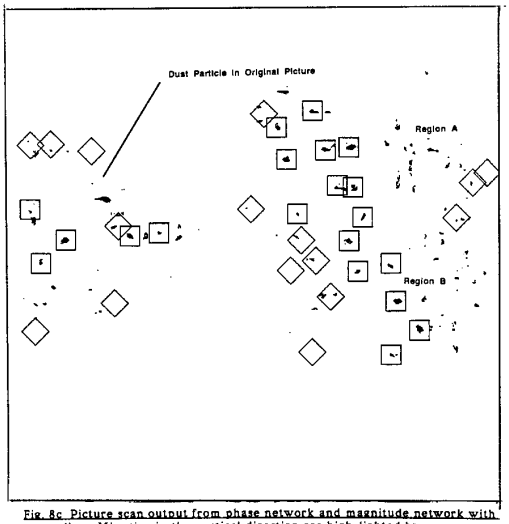

Fig. 8c Picture scan output from phase network and magnitude network with scaling. Minutiae in the vertical direction are high-lighted by squares.
Minutaie in the two adjacent directions are high-lighted by diamonds.

conditions when the picture was taken. Noise in these regions, causing slightly dark and bright fringes, stand out prominently. These fringes, in term, induce false responses in Fig. 7c.

To combat against these false response caused by uneven local lighting condition, the original fingerprint image was filtered again, but besides removing local d.c., scaling was done before each convolution so that the mean absolute deviations of pixel values from their means in all convolution windows were constant (i.e. each window would contain roughly the same amount of energy). The phase of the resulting filtered output will remain unchange. The resulting magnitude of the filtered output is shown in Fig. 8a. Networks were trained with vectors formed using the new magnitude data and the entire magnitude diagram was then scanned by the newly trained network and the result is shown in Fig. 8b. Combining with the phase image, Fig. 8c shows the final result. The performance of the system is very much improved.

6. Conclusions

The problem of minutiae extraction from a noisy, grey-scale fingerprint image is investigated. A representation layer containing fixed weights complex Gabor filters was found to maintain the desired information content while allowing, signal to noise improvement, orientation selectivity and data reduction through subsampling.

The system is able to identify all the minutiae in that particular orientation and gives only few false responses. These false responses mainly come from minutiae in adjacent orientations and from areas in the original image where the signal level is low. Variations in network testing results show that training set selection, as well as subsampling and presentation procedures are important in defining the quality of the resulting network.

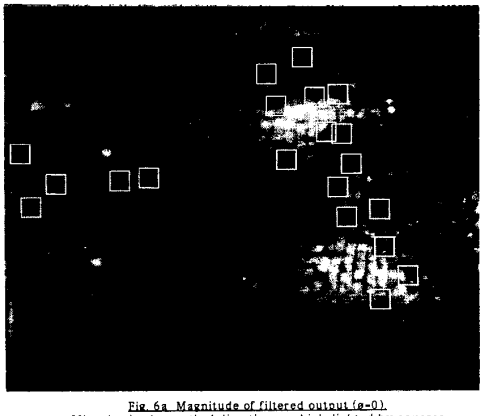

Fig. 6a Magnitude of filtered output (a=0).
Minutiae in the vertical direction are high-lighted by squares

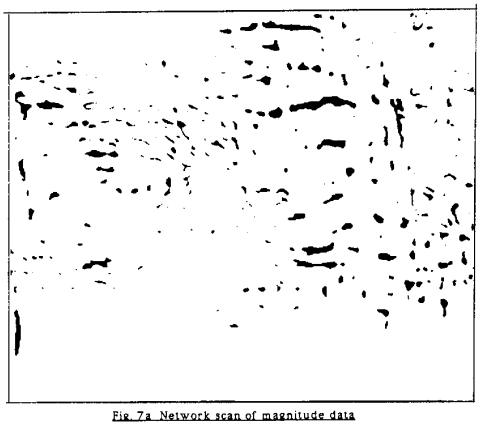

Fig. 7a Network scan of magnitude data

References

[1] **B. Widrow and S.D. Stearns**, Adaptive Signal Processing, Prentice-Hall In., Englewood Cliffs, NJ (1985).

[2] **D. Rumelhart, J. McClelland** and the PDP research group, Parallel Distributed Processing, Explorations in the Microstructure of Cognition, MIT Press, Cambridge, M.A. (1986).

[3] **G. Tesauro and T.J. Sejnowski**, *A 'neural' network that learns to play backgammon*, In D.Z. Anderson, editor, Neural Information Processing System, American Institute of Physics (1988).

[4] **P.M. Sheaand and V. Lin**, *Detection of Explosives in Checked Airline Baggage Using an Artificial Neural System*, Proceedings of IJCNN, II 31-34 Washington, DC (1989).

[5] **R.P. Gorman and T.J. Senjowski**, *Analysis of hidden units in al layered network to classify sonar targets*, Neural Networks, 1,75-79 (1988).

[6] **T.J. Sejnowski and C.R. Rosenberg**, *Parallel Networks that Learn to Pronounce English Text*, Complex System 1, 145-168 (1987).

[7] **B. Denby**, *Neural Network and Cellular Automata in experimental high energy physics*, Computer Physics Communication 49, 429-448 (1988).

[8] **J. Daugman**, *Uncertainty relation for resolutionin space, spatial frequency, and orientation optimized by two-dimensional visual cortical filters*, J. Opt. Soc. Am. A/Vol, No.7, 1160-69 (1985).

[9] **M. Leung and A.M. Peterson**, *Multiple Channel Neural Network Model for Textural Image Segmentation*, submitted to IEEE NIPS Conf., Denver (1990).

[10] **A. Bovik, M. Clark and W. Geisler**, *Computational Texture Analysis Using Localized Spatial Filtering*, Proceedings of Workshop on Computer Vision, Miami Beach, FL, 201 - 206 (1987)

[11] Grey-scale fingerprint data was supplied by H.W. Tomlinson, D. Brown and J. Henkes.

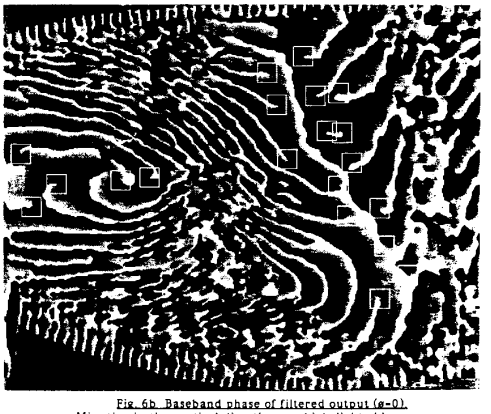

Fig. 6b Baseband phase of filtered output (a=0).
Minutiae in the vertical direction are high-lighted by squares

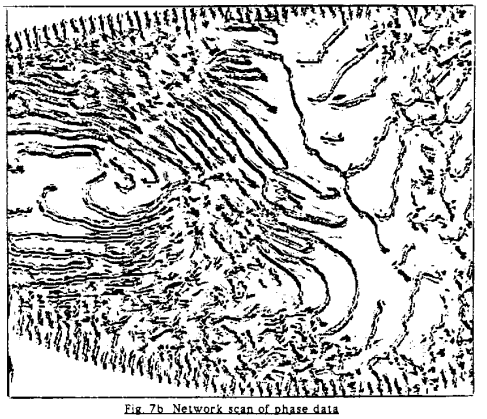

Fig. 7b Network scan of phase data

Preprocessing of Image Window

The fingerprint in Fig. 3 was convolved with the six Gabor filters mentioned above. The resulting filter images shown good enhancement of ridges running in some particular directions as expected. Real and imaginary part of filtered images were stored for further use. Fig. 5 shows the imaginary part of the filtered image using a Gabor filter running in the vertical direction.

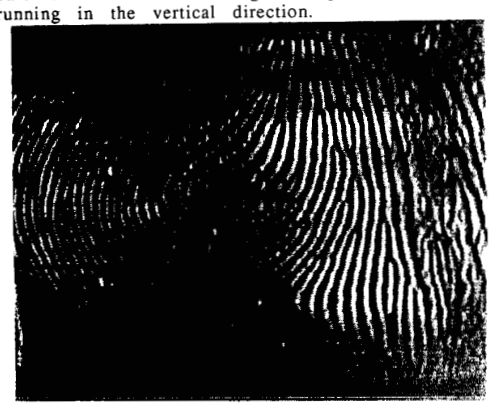

Fig. 5 Imaginary part of the filtered fingerprint image using filter with ø=0

It was observed that the phase was seriously distorted by a ramp-like pattern going across the picture. This distortion is due to the presence of local d.c. in the original image. Going back to Eq. 6, if d.c. is present in t(x,y), c(x,y) and s(x,y) will contain terms involving $\cos(2\pi Fx')$ and $\sin(2\pi Fx')$. This will introduce the ramp-like distortion in the baseband phase. To eliminate this effect, local averages were subtract out of image windows before convolving with the different filters. Additional preprocessing was also done to normalize the signal magnitude in different image windows. This will be discussed later.

Baseband Phase and Magnitude

The resulting baseband phase and magnitude of the filtered fingerprint are shown in Fig 6a and 6b. The minutiae in the vertical direction in Fig 6b. stand out as a dark spot in a generally bright area. In Fig. 6b, minutiae show up at the end of some horizontal edges. These edges are produced by the 2π discontinuities of the phase. The representation layer, therefore clearly preserves the characteristic features of the data. Also, it is clear that both the phase and magnitude data are essentially for the identification of minutiae as each of the two corresponding feature is not confined only to areas around minutiae.

Neural Network Training

It was decided to train the back-propagation network to extract minutiae in the vertical direction (ø = 0). The extraction of minutiae in the other directions and can easily be handled as the presence of rotational symmetry in the case. A complete system, therefore, will consist of six networks each detecting minutiae in their respective directions, followed by a winner-take-all section.

Training sets were composed of samples from minutiae in the vertical directions (50%), samples from minutiae in other directions (15%) and random samples (35%). The size of these sets were 100. The minutiae positions used to make up the training and testing sets were randomly separated to test the generalization properties of these back-propagation networks.

Training was performed with a variety of sub-sampling strategies. Both I and Q filter outputs alone, various combinations magnitude and phase data were used to form training vectors. Networks were trained until 100% convergence was achieved. In order to get convergence, it was often necessary to use a error tolerance method so that only samples giving large output errors were trained. As training progressed, the tolerance was reduced until complete convergence was obtained.

It was discovered that the networks using I and Q signals alone showed poor generalization properties even though all training vectors converged. It appeared that these networks were not able to extract the information identifying minutiae which is embedded in the phase and magnitude of the I and Q signals. So, baseband phase and magnitude data were fed into networks directly. The results were much improved.

It was clear, from observing the weights of networks, that they were actually only using the magnitude information. Those weights connecting the magnitude data had much larger absolute values than those connecting the phase data. This phenomena occurred as the feature identifying minutiae in the magnitude diagram, i.e., dark spot in a bright area, is a much more prominent feature than that the phase edge ending feature of the phase diagram. Networks tended to develop in such a way to concentrate only on magnitude data. Since, it is apparent that both magnitude and phase information is necessary to uniquely identify minutiae (discussed in the last section), it was decided to feed the phase and magnitude data separately into different networks so that phase information can be fully utilized for minutiae identification. The outputs of magnitude and phase networks could then be logically ANDed together for final identification.

When networks were trained by this procedure, the best subsampling strategy for magnitude data was just not appropriate for the phase data. Since the features identifying minutiae in the phase data are edge endings, more samples are required to give high performance networks. Two separate sampling strategies were tried and optimum strategies were obtained for the phase and magnitude networks.

5. Extraction Results and Discussions

Using guidance from the results in the testing sets, the entire magnitude and phase diagram were scanned through by back-propagation networks developed from 5-pt magnitude data and from 25-pt. phase data. Typical resulting images are shown in Fig. 7. Fig. 7a shows the resulting magnitude image for the fingerprint in Fig. 3 whereas Fig. 7b shows the phase image result. To use both phase and magnitude information to identify minutiae, Fig 7a and 7b were thresholded, ANDed to give Fig 7c.

Comparing Fig. 7a and 7b with Fig. 6a and 6b, it appears that the magnitude network picked out, as expected, dark spots in bright area. The phase network actually picked out edges instead of edge endings. This results form the specific training samples used to instruct the network. These training sets contained insufficient non-minutiae edge samples to force the network to look for edge endings rather than the entire edge. Training with additional vectors selected along these edges should correct this difficulty.

As shown in Fig. 7c, after combining the two network outputs, all minutiae in the selected direction (0 degree) are identified. The diagram also shows quite a number of false responses. A substantial percentage of the false responses are caused by minutiae in other closely aligned directions that were not fully filtered by the Gabor filter. As data from only one direction was fed in at present, it would be very difficult for the system to reject minutiae in some adjacent directions. In a complete system, where all directions are represented by their individual networks, these minutiae would be detected in their correct direction. Errors of this type would, therefore, be eliminated in the fusion of the combined results.

The rest of the false responses are concentrated in 3 regions, region A, B and C as shown. Going back to the original fingerprint image (Fig. 3), it was observed that region A is a region where the signal level is high (very bright) whereas B and C are regions where signal level is low (dark). These variations of signal levels are due to the local lighting